J Therm Anal Calorim
DOI 10.1007/s10973-017-6584-x

Spinodal decomposition and martensitic transformation in Cu–Al–Mn shape memory alloy

Diego Velazquez[1,2] · **Ricardo Romero**[1,3]

Received: 29 December 2016 / Accepted: 14 July 2017

Abstract Isothermal treatments at 413 K were performed in Cu–Al–Mn shape memory alloy samples, to study their effects on the martensitic transformation. This procedure, within the miscibility gap, produces spinodal decomposition. After each aging thermal treatment, martensitic transformation was monitored using Differential Scanning Calorimetry (DSC). Spinodal decomposition significantly changes the characteristics of the martensitic transition, reducing the transformed volume and modifying the critical temperatures. Furthermore, transformation hysteresis loop narrows as the volume fraction of the spinodal precipitates increases. Effects of thermal cycling through the martensitic transformation were studied in aged alloy samples. It was found that cycling produces critical temperatures changes, an increase in the transformed volume fraction, and a wider hysteresis loop. The observed results were discussed considering the interaction between spinodal precipitates and martensitic plates.

Keywords Shape memory alloys · Cu–Al–Mn · Spinodal decomposition · Martensitic transformation · Hysteresis

✉ Diego Velazquez
dvelazq@exa.unicen.edu.ar

[1] Instituto de Física de Materiales Tandil (IFIMAT) - UNCPBA, Pinto 399, Buenos Aires, 7000 Tandil, Argentina

[2] Consejo Nacional de Investigaciones Científicas y Técnicas, Godoy Cruz 2290, C1425FQB Buenos Aires, Argentina

[3] Comisión de Investigaciones Científicas de la Provincia de Buenos Aires, Calle 526 e/10 y 11, La Plata, Argentina

Introduction

The Cu–Al–Mn βphase at high temperature has a bcc structure and, under suitable thermal treatments (quenching), can be retained at low temperatures in metastable state. During quenching, the system undergoes two-order transitions namely: $A2 \rightarrow B2$ and $B2 \rightarrow L2_1$. Besides, in the course of cooling, the metastableβ Cu–Al–Mn undergoes a martensitic transformation; a solid-state diffusionless first-order phase transition takes place. Due to cooling, martensite plates of up to 24 different orientations (variants) are induced from a single crystal of the parent phase. The forward (reverse) transformation begins by cooling (heating) at a temperature called M_s (A_s) and finishes at M_f (A_f). These are known as transition characteristic temperatures and are generally strongly dependent on the alloy composition [1].

As in other Cu-based shape memory alloys, a hysteresis loop is formed when temperature changes in a cyclical way throughout the martensitic transformation. This hysteresis loop is one of the essential characteristics of the martensitic transformation and is linked to dissipative mechanisms operating at different spatial scales. Those associated mechanisms are: the nucleation of a new phase and interaction of interfaces with defects (microscopic scale), formation and annihilation of elastically interacting domains (mesoscopic scale) and heat transfer within the sample and between the material and its surroundings (macroscopic scale) [2]. Although there is considerable scatter in the experimental data, a typical thermal hysteresis width, $A_f - M_s$, for thermally induced transformation in Cu–Al–Mn is around 25 K [3, 4]. Interestingly, this hysteresis width is apparently independent on the sample composition, at least for electronic concentrations (e/a) smaller than 1.46, for which a 18R orthorhombic structure is formed after

Published online: 28 July 2017

martensitic transformation [5]. It is worth mentioning that the addition of Mn to Cu-Al alloys significantly modifies the lattice constant. In fact, it has been found that the lattice constant along the $Cu_3Al \rightarrow Cu_2MnAl$ line increases for about 2% [6, 7].

On the other hand, aging βphase at intermediate temperatures, within a miscibility gap, produces spinodal decomposition in a Cu_3Al-rich phase and a Cu_2AlMn-rich phase [6, 8, 9]. Spinodal decomposition produces a two-phase structure with interface planes parallel to {100} planes [8]. In the early stage of decomposition, the lattice constant difference is accommodated by elastic strains in the interfacial plane. However, additional aging causes the loss of the coherence between the two phases and the formation of interfacial dislocations takes place [6–8]. In both cases, a stress elastic field is generated.

As expected, this decomposition has important effects on the martensitic transformation. A very interesting consequence of spinodal decomposition on martensitic transformation in Cu-Mn–Al has been found by Kokorin et al. [10]: aging at 498 K produces a significant reduction of the martensitic transformation hysteresis loop, from 37 to 12 K, after 3 h of thermal treatment. A similar result was reported in Ref. [9]. It is worth noting that narrowing the hysteresis width would be very useful in various applications which make use of the shape memory effect [11–13]. Therefore, knowledge about how the hysteresis width evolves and its associated effects, when the material is thermally treated, have a significant importance.

Although several experimental techniques can be used for characterizing the martensitic transformation, Differential Scanning Calorimetry (DSC), with suitable calibrations [14] and appropriate data-processing mechanism [15, 16], provides one of the most accurate determinations of temperatures and energy dissipation for thermally induced martensitic transformation [17].

In the present work, we study the effects of isothermal aging, within the temperature range of spinodal decomposition, on the martensitic transformed volume fraction, characteristics temperatures and hysteresis in a β Cu–Al–Mn alloy. Also, the evolution of transition temperatures, latent heat, entropy and transformation kinetics in aged samples under thermal cycling are reported.

Experimental

The 71.66 at. % Cu–20.12 at. % Al-8.22 at. % Mn (nominal composition) alloys with electronic concentration $e/a = 1.40$ were prepared by melting about 15 g of 4 N purity elements in an arc furnace under partial Ar atmosphere using a non-consumable tungsten electrode and were turned and re-melted several times in order to improve their homogeneity. The resulting ingots were homogenized by annealing at 1123 K during 24 h in a resistive furnace. Slices of 5 mm thickness were cut from ingots. The slices were hot-rolled at 1073 K up to 1.5 mm thickness, and quenched in water at room temperature. The resulting microstructure consists of polycrystals with grain size around 3–4 mm. Samples of 4×4 mm^2 for Differential Scanning Calorimetry (DSC) were cut using a low-speed diamond saw. Before each test, the samples were treated in β phase at 1073 K for at least 900 s, then quenched in an ice–water mixture (273 K) to retain metastable β phase, and later aged at room temperature ($\sim$295 K) for 24 h. This aging was made in order to reduce the vacancy concentration retained by quenching. This procedure will be called hereafter "Basic Heat Treatment" (BHT). Calorimetric measurements were taken using a highly sensitivity differential scanning calorimeter Setaram 131 Evo DSC, specially designed for studying solid–solid phase transitions, at constant scanning rate (10 K min^{-1}). The scan rate, the sample's shape and volume, were kept approximately constant (within experimental conditions). This was done in order to avoid spurious contributions associated with heat transfer between the specimen and its surroundings [17]. Moreover, before each test, the sample was mechanically polished with sandpaper (grit 600) and chemically etched by immersion in a solution of 50% HNO_3 in H_2O during $\sim$15 s in order to optimize the contact between the sample and the calorimeter's aluminum crucible. Samples with BHT were isothermally aged in a resistive furnace at temperature, $T_{iso} = 413$ K, for different times t_{ag}, 0 h $< t_{ag} <$ 300 h.

Results

The baseline-corrected DSC curves recorded during forward (exothermic, $dQ/dT < 0$) and reverse (endothermic, $dQ/dT > 0$) martensitic transformation of samples with BHT, and after aging for 90 h at 413 K, are shown in Fig. 1. Critical temperatures were determined using the transformed volume fraction as a function of temperature: on cooling, the temperature at which 1% (99%) of the martensite has grown was defined as M_s (M_f) and equivalently for the β phase on heating for A_s (A_f) [18]. It can be noticed that in both cases the phase change is characterized by smooth peaks, without heat exchange jumps.

As shown in Fig. 1, heat treatment at 413 K considerably modifies the transformation characteristics: transition characteristic temperatures are increased, the peaks are flattened and the area under the peaks decreases. Moreover, the phase change temperature interval ($M_s - M_f$ or $A_f - A_s$) increases considerably and the hysteresis loop narrows, being measured as:

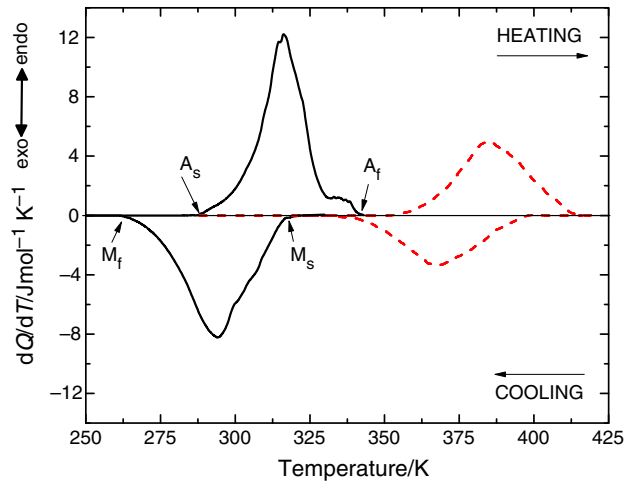

Fig. 1 Baseline-corrected DSC curves, corresponding to forward and reverse martensitic transformation for BHT samples (*left, black line*), and after aging 90 h at 413 K (*right, red dashed line*)

$$\Phi = A_f - M_s. \quad (1)$$

Evolution of the hysteresis for different aging times at 413 K is shown in Fig. 2. It is noted that the decrease in hysteresis at the beginning of the aging is fast, but after 90 h becomes considerably slower, tending to a limit value. Taking into consideration the relatively large grain size, for BHT samples it is reasonable to approximate the equilibrium temperature as [19]:

$$T_0 = (A_f + M_s)/2. \quad (2)$$

However, for spinodally decomposed samples, their complex microstructure must be taken into account. In light of this, we define a temperature

$$\theta_0 = (A_f + M_s)/2, \quad (3)$$

which matches T_0 only for BHT samples. A clear increase in θ_0 as a function of aging time is observed in Fig. 2. This observed increase can be partially explained by the composition change in the matrix phase due to the spinodal decomposition. Amid this process, the matrix phase becomes impoverished in Mn and Al, although to a lesser extent in the latter element [8]. Moreover, as it is mentioned above, the microstructure resulting from the spinodal decomposition can affect the θ_0 value. The hysteresis behavior will be discussed exhaustively later.

The transformation entropy change was determined from curves for the forward (reverse) transformation as follows [20, 21]:

$$\Delta S^{\beta\to m(m\to\beta)} \cong \int_{M_s(A_s)}^{M_f(A_f)} \frac{1}{T}\frac{dQ}{dT}dT. \quad (4)$$

It should be noted that (4) is calculated assuming that the whole mass of the sample transforms. This is only true for samples which underwent the BHT, and in this case, we named it ΔS_0. For aged samples, instead, ΔS must be interpreted as the apparent entropy change. For all cases, the values reported were calculated as the average of the absolute values obtained for the forward and reverse transformations from Eq. 4.

BHT samples obtained a value of $\Delta S_0 = 1.27$ Jmol^{-1}K^{-1}, satisfactorily matching those reported [4, 5]. Apparent ΔS values for samples aged at 413 K as a function of thermal treatment time are shown in Fig. 3. It becomes clear that the apparent entropy change decreases strongly with aging time.

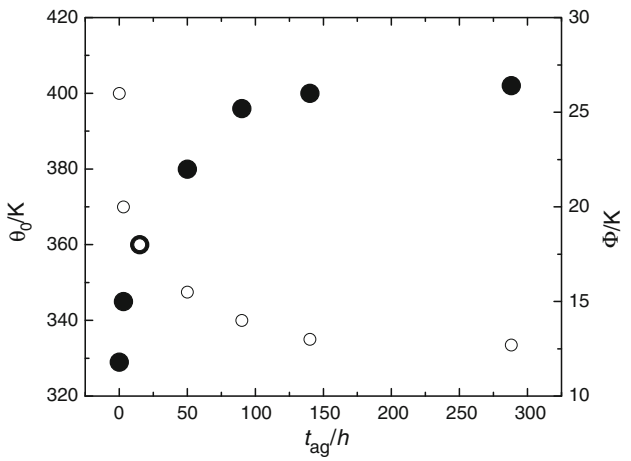

Fig. 2 Evolution of θ_0 (*filled circle*) and hysteresis Φ (*unfilled circle*) as function of aging time at 413 K

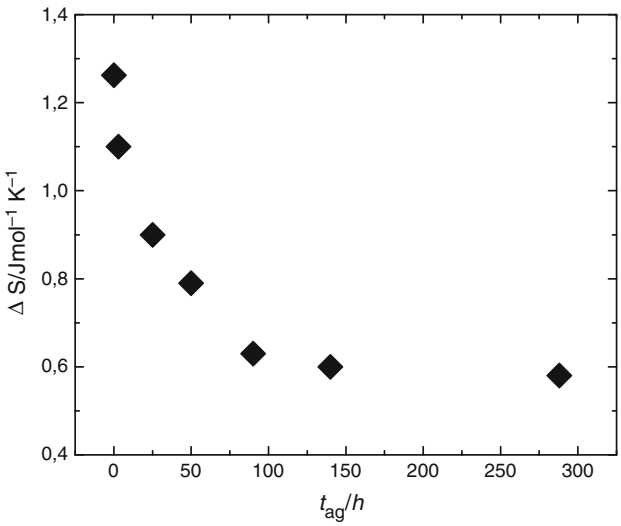

Fig. 3 Apparent transformation entropy ΔS for samples aged at $T_{iso} = 413$ K as function of aging time (t_{ag})

With the aim of investigating the stability of the thermal hysteresis narrowing, thermal cycling between room temperature (293 K) and 410 K on aged samples was performed, and its effect analyzed. Using a scanning rate of 10 K min^{-1}, the time spent at high temperatures is short, and the cycling thermal treatment does not modify the volume fraction of spinodal decomposition for long time aged samples. Cycling effects on samples aged 90 h at 413 K are shown in curves of Fig. 4.

From Figs. 5 and 6, it becomes clear that the thermal cycling on aged samples has significant effects on the martensitic transformation behavior. The temperature θ_0 decreases approximately 7 K after 10 cycles, while the apparent entropy changes 24% and the hysteresis increase 4 K. It is worth mentioning that cycling has no appreciable effect on the BHT samples. Figure 7 shows the apparent stored elastic energy of forward and reverse martensitic transformation as a function of the cycle number, n. These results will be discussed later.

Discussion

Precipitates can have different effects on thermally induced martensitic transformations [22]. In Cu-Al-Ni, the introduction of γ-type precipitates increases transformation temperatures, and can even change the type of martensite formed from 2H to 18R, which reduces the hysteresis cycle width [23, 24]. In Cu-Al–Be, γ_2 precipitates increase transformation temperatures, whereas the hysteresis width apparently does not change [25]. In Cu–Zn-Al, the presence of γ precipitates modifies transformation characteristic temperatures and causes a wider hysteresis loop, due to plastic accommodation and relaxation processes associated with matrix shape change upon transformation [26–30]. In addition, thermal cycling produces stability of the transformation temperatures for dense distributions of small precipitates and, for bigger sized precipitates, an increase in the transformation temperatures plus a reduction of the hysteresis width [31]. It is noteworthy that the results obtained in this work differ considerably from those mentioned above.

As it has been pointed out previously, aging of the metastable βphase within the miscibility gap produces spinodal decomposition into a Cu_2MnAl-rich phase and a Cu_3Al-rich phase [8]. As expected, this process has important effects on the martensitic transformation. The overall transformation cycle characteristics change, as can be seen in Figs. 1–3. Due to its composition, Cu_2MnAl-like particles cannot undergo martensitic transformation [4]. Additionally, it is known that for Cu–Al–Mn with $e/a < 1.46$, the composition effect on the martensitic

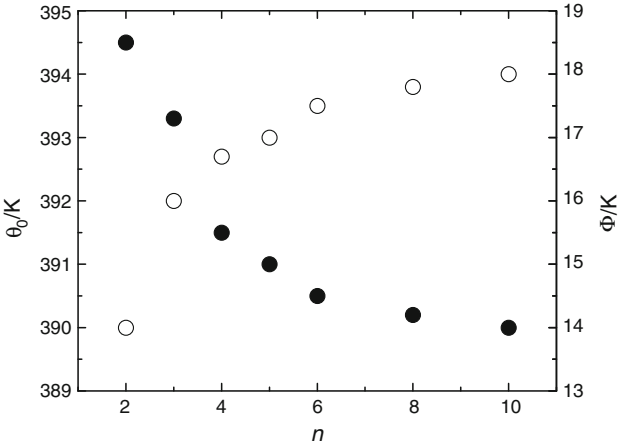

Fig. 5 Evolution of θ_0 (*filled circle*) and hysteresis Φ (*unfilled circle*) as a function of cycle number, for samples aged 90 h at 413 K

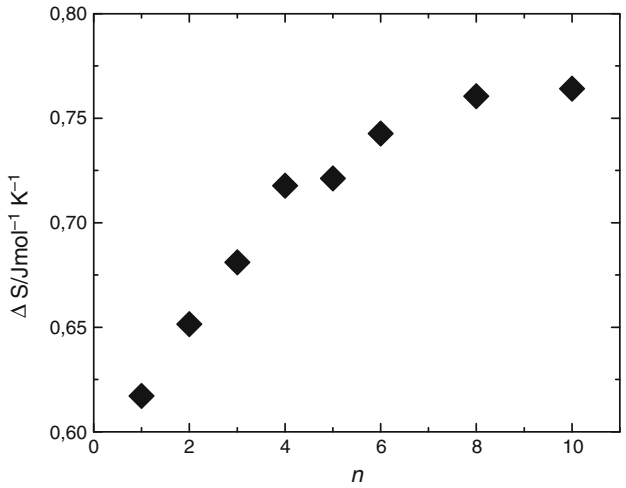

Fig. 6 Apparent entropy change ΔS as a function of cycle number, for samples aged 90 h at 413 K

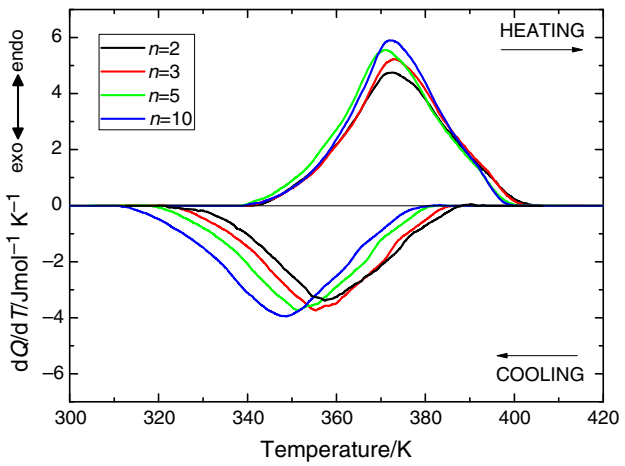

Fig. 4 Curves corresponding to forward and reverse martensitic transformation for samples aged 90 h at 413 K. Cycles 2 to 10

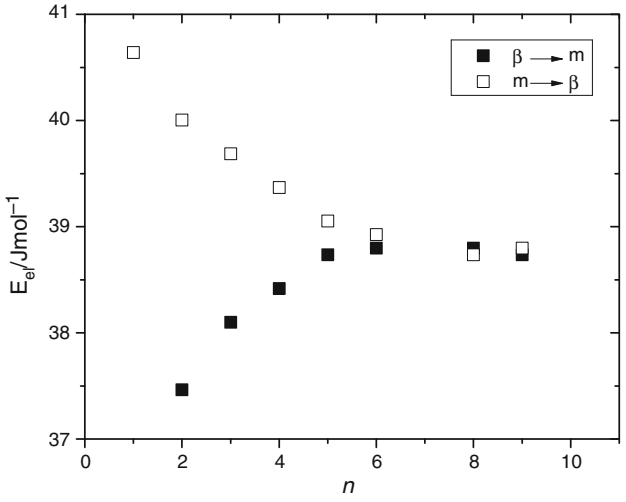

Fig. 7 Stored elastic energy: $E_{el}^{\beta\to m} = {}^1\!/_2\,(M_f - Ms)\Delta S_0$ (*filled square*) and $E_{el}^{m\to\beta} = {}^1\!/_2\,(A_{lf} - A_s)\Delta S_0$ (*unfilled square*), as a function of the cycle number, for samples aged 90 h at 413 K

transformation entropy change is small [5]. From experimental data of Fig. 3, by using entropy's extensivity, the transformed volume fraction evolution can be estimated as:

$$f_v(\%) = \frac{\Delta S}{\Delta S_0} \times 100. \tag{5}$$

After $t_{ag} = 130$ h, this transformed volume fraction is reduced to $\sim$45%. On the other hand, a shift toward higher values in θ_o is observed in Fig. 2. This shift could be due to, at least partially, the composition change of the sample fraction that can undergo a martensitic transformation. The θ_0 behavior will be discussed in detail later.

On the other hand, the energy dissipated (E_{diss}) in a hysteresis cycle can be estimated by means of [32]:

$$E_{diss} = \Phi\Delta S_0. \tag{6}$$

Present results show that $E_{diss} = 34.3$ J mol^{-1} for BHT samples, and it is reduced to $E_{diss} = 16.5$ J mol^{-1} for 90 h aged samples at 413 K, due to the narrowing of Φ. This behavior has been attributed to relaxation phenomena [10]. Given the interaction of martensite plates with spinodal decomposition precipitates, relaxation processes undoubtedly must take place. Nevertheless, by reason of the results, it becomes necessary to explain the process thoroughly.

Since the martensite can be stress induced, it is quite possible that the above-mentioned elastic stress field due to interfaces affect the martensitic transformation, generating the formation of a limited number of variants. With a limited variants number, the interaction between variants is reduced. As a result, the hysteresis cycle width diminishes. This may be the cause of observed hysteresis narrowing in the aged samples.

However, the cycling results (see Figs. 4–6) show that that the effects of aging are not permanent. Namely, as we increase the number of cycles it can be observed that: θ_0 decreases, Fig. 5; the hysteresis width increases, Fig. 5; and the apparent entropy change increases, Fig. 6. These findings can be rationalized as follows: although the number of variants has been reduced, the induced variants can interact with the spinodal precipitates during cycling. As a consequence of this interaction, the martensite plates are plastically deformed. This process is possible since the plastic deformation stress of martensite is relatively low [33], while the plastic deformation stress of Cu_2AlMn is high [34]. The martensite plastic deformation causes, progressively, a relaxation of the elastic stress field, allowing the appearance of new variants of martensite. The increase in the number of variants permits to transform a larger volume of the sample, see Fig. 6. In addition, building up the number of induced variants raises variant to variant interaction and, thus, the hysteresis width, Fig. 5. Since the cycling does not modify the composition of the martensitically transformed sample fraction, the elastic stress field relaxation also consequently decreases θ_0, see Fig. 5.

Thermodynamic considerations establish that calorimetrically measured heat comes from two contributions, namely latent heat and stored elastic energy [35–37]. Explicitly:

$$-\left|Q_F\right| = -|H_{\beta\to m}| + \left|E_{el}^{\beta\to m}\right|, \tag{7}$$

$$|Q_R| = |H_{m\to\beta}| - |E_{el}^{m\to\beta}|, \tag{8}$$

where Q_F and Q_R are the heat released or absorbed, $H_{\beta\to m}$ and $H_{m\to\beta}$ are chemical enthalpy changes (or latent heat), and $E_{el}^{\beta\to m}$ and $E_{el}^{m\to\beta}$ are the stored and released elastic energy during forward and reverse transformations, respectively. Since in this work, the critical transformation temperatures are above 273 K, and a specific heat difference $\Delta C_p^{\beta\to m} \sim 0$ is considered [38].

There is interesting evidence of plastic deformation in the martensite plates. Indeed, according to references [37, 39], the maximum amount of energy that could be stored elastically in forward transformation is:

$$E_{el}^{\beta\to m} = {}^1\!/_2(M_s - M_f)\Delta S_0. \tag{9}$$

Similar considerations lead to a maximum energy released in reverse transformation:

$$E_{el}^{m\to\beta} = {}^1\!/_2(A_s - A_f)\Delta S_0. \tag{10}$$

It is important to mention that in both cases the actual value can be lower, and part of the apparent elastic energy (stored or released) could correspond to frictional effects, irreversibly dissipated as heat, such as in the case of plastic deformation. Therefore, the E_{el} values must be understood

as an upper bound [37]. Figure 7 shows $E_{el}^{\beta\rightarrow m}$ and $E_{el}^{m\rightarrow\beta}$ as a function of cycle number. It follows that, at the beginning of the cycling $E_{el}^{m\rightarrow\beta}$ values are higher than $E_{el}^{\beta\rightarrow m}$ ones; however, after about six cycles, the values converge. It is known that the martensite plastically deformed has a tendency to be retained in the reverse transformation [35]. This martensite pinning leads to an increase in the $(A_f - A_s)$ temperature interval. Therefore, the results of Fig. 7 indicate a progressive plastic deformation of the martensitic phase.

Conclusions

The effects of intermediate temperature thermal aging in β Cu-20.12 at.% Al-8.22 at.% Mn samples were investigated using DSC. The main results are:

- Aging at 413 K, within the miscibility gap, gradually induces samples spinodal decomposition.
- The spinodal decomposition has important effects on the martensitic transformation: The transformed volume is reduced, characteristic temperatures change and the hysteresis loop narrows.
- The reduction in the number of martensite variants which are able to form can explain the hysteresis loop narrowing.
- Thermal cycling through the martensitic transformation of aged samples partially modifies the above effects: Transformed volume increases, critical temperatures decreases and the hysteresis loop widens.
- Interaction between martensite plates and precipitates lead to plastic deformation of the martensite, this process could explain the whole observed results.

Acknowledgements This work has been carried out with the financial support of the CONICET, ANPCYT, SECAT-UNCPBA and CICPBA, Argentina. We are grateful for our fruitful discussions with our colleague Dra. A. Cuniberti and her critical reading of this paper's manuscript. The authors acknowledge O. Toscano and E. Portalez for their contributions to the experimental work.

References

1. Ahlers M. Martensite and equilibrium phases in Cu-Zn and Cu-Zn-Al alloys. Prog Mater Sci. 1986;30:135–86.
2. Ortín J, Delaey L. Hysteresis in shape-memory alloys. Int J Non Linear Mech. 2002;37:1275–81.
3. Mallik US, Sampath V. Effect of alloying on microstructure and shape memory characteristics of Cu–Al–Mn shape memory alloys. Mater Sci Eng, A. 2008;481–482:680–3.
4. Prado MO, Decorte PM, Lovey FC. Martensitic transformation in Cu-Mn-Al Alloys. Scr Metall Mater Mater. 1995;33:877–83.
5. Obradó E, Mañosa L, Planes A. Stability of the bcc phase of Cu-Al-Mn shape-memory alloys. Phys Rev B. 1997;56:20–3.
6. Kainuma R, Satoh N, Liu XJ, Ohnuma I, Ishida K. Phase equilibria and Heusler phase stability in the Cu-rich portion of the Cu–Al–Mn system. J Alloys Compd. 1998;266:191–200.
7. Bouchard M, Livak RJ, Thomas G. Interphase interfaces in spinodal alloys. Surf Sci. 1972;31:275–95.
8. Bouchard M, Thomas G. Phase Transitions and Modulated Structures in Ordered $(Cu\text{-}Mn)_3Al$ Alloys. Acta Metall. 1975;23:1485–500.
9. Marcos J, Mañosa L, Planes A, Romero R, Castro ML. Kinetics of the phase separation in Cu–Al–Mn alloys and the influence on martensitic transformations. Philos Mag. 2004;84:45–68.
10. Kokorin VV, Kozlova LE, Titenko AN. Temperature hysteresis of martensite transformation in aging Cu-Mn-Al alloy. Scr Mater. 2002;47:499–502.
11. Aslani H, Cabrera C, Rahnama M. Potential of Cu-Al-Mn alloys bars for seismic applications. Earthq Eng Struct Dyn. 2012;41:1549–68.
12. O'Brien B, Bruzzi M. Shape Memory Alloys for use in medicine. Compr. Biomater. Vol. 1. Elsevier Ltd.; 2011.
13. Oliveira JP, Panton B, Zeng Z, Omori T, Zhou Y, Miranda RM, et al. Laser welded superelastic Cu-Al-Mn shape memory alloy wires. Mater Des. 2016;90:122–8.
14. Pishchur DP, Drebushchak VA. Recommendations on DSC calibration. J Therm Anal Calorim. 2016;124:951–8.
15. Kato H, Sasaki K. Avoiding error of determining the martensite finish temperature due to thermal inertia in differential scanning calorimetry : model and experiment of Ni–Ti and Cu–Al–Ni shape memory alloys. J Mater Sci. 2012;47:1399–410.
16. Pelegrina JL, Torra V. Comment on "Effects of heat-flux features on the differential scanning calorimetry curve of a thermoelastic martensitic transformation" by Benke et al. [Mater Sci Eng A 481-482 (2008) 522]. Mater Sci Eng A 2010;527:2437–40.
17. Lohan NM, Pricop B, Burlacu L, Bujoreanu L-G. Using DSC for the detection of diffusion-controlled phenomena in Cu-based shape memory alloys. J Therm Anal Calorim. 2016. doi:10.1007/s10973-016-5926-4.
18. Pelegrina JL, Romero R. Calorimetry in Cu–Zn–Al alloys under different structural and microstructural conditions. Mater Sci Eng, A. 2000;282:16–22.
19. Salzbrenner RJ, Cohen M. On the thermodinamics of thermoelastic martensitic transformations. Acta Metall. 1979;27:739–48.
20. Planes A, Romero R, Ahlers M. Thermal properties of the martensitic transformation of Cu-Zn and Cu-Zn-Al shape memory alloys. Scr Metall. 1989;23:989–94.
21. Bachaga T, Rekik H, Krifa M, Suñol JJ, Khitouni M. Investigation of the enthalpy/entropy variation and structure of Ni–Mn–Sn (Co, In) melt-spun alloys. J Therm Anal Calorim. 2016. doi:10.1007/s10973-016-5716-z.
22. de Castro Bubani F, Lovey FC, Sade ML. A short review on the interaction of precipitates and martensitic transitions in CuZnAl shape memory alloys. Funct Mater Lett. 2017;10:1740006.
23. Zárubová N, Gemperle A, Novak V. Initial stages of y2 precipitation in an aged Cu-Al-Ni shape memory alloy. Mater Sci Eng, A. 1997;222:166–74.
24. Araujo VEA, Gastien R, Zelaya E, Beiroa JI, Corro I, Sade M, et al. Effects on the martensitic transformations and the microstructure of CuAlNi single crystals after ageing at 473 K. J Alloys Compd. 2015;641:155–61.
25. Cuniberti A, Montecinos S, Lovey FC. Effect of γ_2-phase precipitates on the martensitic transformation of a β-CuAlBe shape memory alloy. Intermetallics. 2009;17:435–40.
26. Pons J, Portier R. Accommodation of γ-phase precipitates in Cu-Zn-Al shape memory alloys studied by high resolution electron microscopy. Acta Mater. 1997;45:2109–20.
27. Pons J, Cesari E. Precipitates in β Cu-Zn-Al: Iinfluence on Martensitic Transformations. Thermochim Acta. 1989;145:237–43.

28. Lovey FC, Torra V, Isalgué A, Roqueta D, Sade M. Interaction of single variant martensitic transformation with small γ type precipitates in CuZnAl. Acta Metall Mater. 1994;42:453–60.
29. Lovey FC, Torra V. Shape memory in Cu-based alloys: phenomenological behavior at the mesoscale level and interaction of martensitic transformation with structural defects in Cu-Zn-Al. Prog Mater Sci. 1999;44:189–289.
30. Auguet C, Cesari E, Rapacioli R, Mañosa L. Effect of γ precipitates on the martensitic transformation of β CuZnAl studied by calorimetry. Scr Metall. 1989;23:579–83.
31. Pons J, Cesari E. Martensitic Transformation Cycling in a β Cu-Zn-Al Alloy Containing γ-Precipitates. Acta Met Mater. 1993;41:2547–55.
32. Liu Y, McCormick PG. Thermodynamic analysis of the martensitic transformation in NiTi-I. Effect of heat treatment on transformation behaviour. Acta Metall Mater. 1994;42:2401–6.
33. Cuniberti A, Romero R, Ahlers M. The plastic deformation of long range ordered 18R martensitic single crystals of Cu-Zn-Al alloys. Scr Metall Mater. 1992;26:495–500.
34. Umakoshi Y, Yamaguchi M, Yamane T. Deformation and fracture behaviour of the alloy Cu_2MnAl single crystals. Acta Metall. 1984;32:649–54.
35. Cuniberti A, Romero R. Differential scanning calorimetry study of deformed Cu-Zn-Al martensite. Scr Mater. 2004;51:315–20.
36. Yawny A, Lovey FC, Torra V. Entropy production in single-crystal single-interface martensite transformation. Scr Metall Mater. 1995;32:439–44.
37. Wollants P, Roos JR, Delaey L. Thermally and stress-induced thermoelastic martensitic transformations in the reference frame of equilibrium thermodynamics. Prog Mater Sci. 1993;37:227–88.
38. Lashley JC, Drymiotis FR, Safarik DJ, Smith JL, Romero R, Fisher RA, et al. Contribution of low-frequency modes to the specific heat of Cu-Zn-Al shape-memory alloys. Phys Rev B. 2007;75:64304.
39. Tuncer N, Qiao L, Radovitzky R, Schuh CA. Thermally induced martensitic transformations in Cu-based shape memory alloy microwires. J Mater Sci. 2015;50:7473–87.